Scanning Microscopy

Volume 10 | Number 2 Article 10

2-7-1996

Formation of Hydrated Calcium Oxalates in the Presence of Poly-L-Aspartic Acid

Jeffrey A. Wesson
The Medical College of Wisconsin, Milwaukee

Elaine Worcester
The Medical College of Wisconsin, Milwaukee

Scanning Microscopy, Vol. 10, No. 2, 1996 (pages 415-424) 1051-6794/96$5.00+.25
Scanning Microscopy International, Chicago (AMF O'Hare), IL 60666 USA

FORMATION OF HYDRATED CALCIUM OXALATES IN THE PRESENCE OF POLY-L-ASPARTIC ACID

Jeffrey A. Wesson* and Elaine Worcester

Zablocki VA Medical Center and The Medical College of Wisconsin, Milwaukee, WI

(Received for publication July 17, 1995 and in revised form February 7, 1996)

Abstract

The effect of poly-L-aspartic acid (PA) on the crystal structure of calcium oxalate crystals grown after spontaneous nucleation was evaluated as a function of relative supersaturation and calcium:oxalate ratio in a buffered salt solution, with pH and ionic strength in the range of normal human urine. PA was used as a model for naturally occurring acidic urine proteins that have been shown to inhibit nucleation and growth of calcium oxalate crystals. The crystals grown were characterized by optical microscopy and X-ray powder diffraction. It was observed that calcium oxalate monohydrate was the preferred crystalline form in the absence of added PA, and it was the only crystalline form obtained at most conditions tested without PA. However, the presence of PA favored the formation of calcium oxalate dihydrate crystals, when present in adequate quantities. The quantity of PA required to affect this change in preferred crystal structure was increased at higher supersaturations and at lower calcium:oxalate ratios, exhibiting a non-linear dependence on both variables. PA was also shown to be a kinetic inhibitor of calcium oxalate dihydrate crystallization. Aspartic acid monomer was found to cause no change in the preferred structure of calcium oxalate monohydrate at mass concentrations well beyond those required with PA to obtain 100% calcium oxalate dihydrate, indicating the critical importance of the polymeric nature of PA for this effect on crystal structure.

Key Words: Calcium oxalate, polyaspartic acid, nephrolithiasis, crystal inhibitors, crystal morphology, crystallization.

*Address for correspondence:
Jeffrey A. Wesson
Zablocki VA Medical Center (111K),
5000 West National Avenue,
Milwaukee, WI 53295
Telephone number: (414) 384-2000 ext. 2825
FAX number: (414) 383-8010
E.mail: jwesson@post.its.mcw.edu

Introduction

Conditions affecting the crystallization of calcium oxalate (CaOx) in ionic solution are of critical importance for understanding nephrolithiasis (kidney stone disease) since CaOx is the dominant species found in these pathologic crystals [13, 14, 17]. One of the principle questions in nephrolithiasis is by what mechanism does the incipient crystal become trapped in the kidney, forming a symptomatic stone. Given the kinetic limitation to stone formation by normal urine flow, a crystal must either evolve rapidly through a combination of nucleation, growth and aggregation to yield a crystal mass that is large enough to become physically trapped in the collecting system or adsorb to the tubular cell surface to allow prolonged crystal mass accumulation [4]. CaOx crystals are commonly found as either the monohydrate (COM) or the dihydrate (COD) structure in patient samples [13, 14, 17]. The structural difference may play a key role in the regulation of nephrolithiasis, although no mechanism for such an effect has yet been established.

Data from several experiments suggest that COM may have a greater tendency to form kidney stones than COD. Previous studies of samples from patient have shown that kidney stones are predominately COM, although COD crystals are also observed [13, 14, 17]. On the other hand, asymptomatic crystals in the urine are usually COD, with COM found in some samples [6]. Laboratory experiments have shown that COM does bind to inner medullary tubular cell membranes [15, 22], although similar experiments have not been published for COD. Other experiments in the same laboratory demonstrate a stronger biological membrane interaction for COM in its greater ability to lyse red blood cells compared to COD [21]. In addition, theoretical calculations of the degree of dimensional matching between crystal lattice structures and head (charge) group distributions of phospholipid membranes show a greater number of matches with COM than with COD crystals [12]. These varied results argue strongly for the possibility that the formation of COD is protective against stone disease, and the most likely mechanism for this effect would be

reduced cell adhesion to the renal tubular cells. Therefore, it is important to understand the conditions that favor COD formation.

Recently, there has been a lot of interest in urinary molecules that have been shown to inhibit CaOx crystal formation [4, 8] and thereby prevent crystal entrapment by limiting crystal size. Many of these molecules have also been shown to influence the crystal structure, leading to the formation of COD rather than COM in typical ionic solutions. Martin *et al.* [16] have shown that both small molecule and macromolecule inhibitors found in urine favor the formation of COD, and the unseparated solutes from urine were more effective in this regard than any of the single component inhibitors tested. The small molecule inhibitors of citrate and pyrophosphate accounted for less than half of the effect noted in the urine solute samples. The known macromolecules tend to be polyanions and are generally acidic in nature [7, 18]. One such macromolecule found in human urine is uropontin [18, 24], which has been shown to be an effective inhibitor of nucleation [23] and growth [24] of CaOx crystals. Uropontin (or osteopontin) is a 44 kDa protein [3], and occurs in rodent urine at a concentration of about 8 μg/ml [5]. It contains 15-20% aspartic acid units [5, 18, 24], including a run of 8-10 aspartic acid units [5, 24], which is thought to be important to crystal surface interactions, possibly in a specific manner [1, 2].

In the experiments described below, we explore the effect of poly-L-aspartic acid (PA) on the structure of CaOx crystals grown by spontaneous nucleation in ionic solution at conditions of pH and ionic strength typical of normal urine samples. The effect of PA on CaOx crystal structure is examined as a function of supersaturation (SS) and calcium:oxalate (Ca:Ox) ratio in order to characterize the phase diagram for this precipitation. PA has been shown to be an effective kinetic inhibitor of CaOx crystallization [11, 24], and specifically should be a convenient, inexpensive model for osteopontin. Due to the dependence of nucleation rate on SS, the effective number of growing particles should increase with SS, and hence, the inhibitor requirement should also increase. The second independent parameter of Ca:Ox ratio has been infrequently studied *in vitro*, but it will certainly influence surface charge densities of crystals and polyelectrolytes and, therefore, their interaction. Most experiments have been done under either equimolar conditions or fixed non-stoichiometric ratios and do not elucidate the dependence on Ca:Ox ratio. Normal human urine has a significant excess of Ca ion with a Ca:Ox ratio in the range of 6:1 to 10:1 [17]. An even wider range of ratios is seen when pathologic states are included.

Materials and Methods

All chemicals were reagent grade and were used without further purification. Solutions were prepared in water that was deionized and filtered using the Nanopure system (Barnstead, Div. Sybron, Boston, MA). Crystals were grown in an ionic buffer solution of 0.15 M NaCl and 0.01 M HEPES (N-[2-Hydroxy]piperazine-N'-[2-ethanesulfonic acid]) titrated to pH 7.5 with HCl. Solutions were prepared by volumetric additions of stock solutions to the appropriate quantity of deionized water. All solutions were equilibrated to room temperature before mixing. Calcium ion was added by volumetric addition of a 10 mM $CaCl_2$ stock solution. Oxalate ion was introduced from a 10 mM stock solution of $Na_2C_2O_4$. Typically, solutions were prepared to a total volume of 10 ml in a new glass scintillation vial. Before Ox ion addition, all other components, including any inhibitors, were added to the container and thoroughly mixed. Immediately following the addition of oxalate ion, the solutions were shaken vigorously for 10 to 15 seconds, and the precipitation was then allowed to occur at room temperature (295 K $\pm$ 3 K) under quiescent conditions. {Authors' note: Subsequent experiments have shown a dependence of the concentration of PA required to obtain COD on the lot of glass vials used for the experiment. This presumably resulted from differences in PA surface adsorption to the different glass vials, but we could eliminate this effect by pretreating the vials with Gel Slick® (AT Biochem, Malvern, PA)}.

PA (Sigma, St. Louis, MO; molecular weight: 15 kDa) was added from a 0.138 mg/ml (9.23 μmolar) stock solution again by volumetric addition. The volume of inhibitor solution added was in excess of the 10 ml total volume described above, and ion and inhibitor concentrations were corrected for this additional dilution. The maximum change was 6.6% at the largest PA levels; however, for all but a few samples, this change was less than 3%. Aspartic acid monomer (Na salt; Sigma) was prepared as an aqueous stock solution at the same mass concentration as PA and added in the same way.

Samples were generally allowed to precipitate for more than 3 hours or until an appreciable crystal mass was observed, before examining the resulting crystals. At the lowest supersaturations, the precipitations required 1 to 2 days before satisfying the latter requirement. No effort was made to verify the completeness of the precipitation, but no difference was observed morphologically between crystals formed early in the precipitation reaction and those formed later, at several conditions. At the highest supersaturations, > 15, there was visible crystal mass within one minute after addition of Ox to the solution. Results for these conditions have been included below for completeness, but we are concerned that the results for those conditions may have been influenced by locally high concentrations of reagents, because of the limitations of mixing technique.

Crystals were isolated from solution by filtering through PCTE (track-etched polycarbonate) filters (5.0 μm pore size, Poretics, Livermore, CA) in Swinney filter holders (Millipore, Bedford, MA). Filters were then placed on a microscope slide with a drop of solution and covered with a cover slide. Optical microscopy was performed immediately on all samples using a Nikon Optiphot-2 microscope (Nikon, Inc., Instrument Group, Melville, NY), and photographs were taken of selected samples with the attached camera system (Olympus Automatic Photomicrographic System PM-10ADS, Olympus Optical, Ltd., Tokyo, Japan). An effort was made to examine the crystals over the entire area of each slide by manually raster scanning the field because the relative quantities of COM and COD crystals sometimes varied from one field to another. At the lowest supersaturations, hundreds to thousands of crystals were seen in each slide. Samples at supersaturations of 7 to 10 formed tens of thousands of crystals. For high supersaturation conditions, where an even larger crystal mass was formed, dense piles of crystals were frequently seen. The edges of such piles were examined thoroughly, but no effort was made to disperse these piles.

Crystal mass determinations were made on some samples by filtering multiple, identically prepared samples and weighing the recovered crystal mass on an XA-200DS analytical balance (Fisher Scientific, Pittsburgh, PA). Filters used were the 5.0 μm PCTE filters as above and 0.1 μm PCTE filters from the same manufacturer. After filtering the crystals and removing excess solvent by pushing a small quantity of air through the pre-weighed filters, the samples were further dried at 323 K for one hour. No change in crystal morphology was noted with this drying protocol. Filter masses were 1.66 mg (standard deviation, SD, 0.05) and 0.89 mg (SD 0.05) for the 5.0 μm and 0.1 μm filters, respectively. Standard deviation (SD) for repeated mass determination of a single filter was also 0.05 mg.

Ca ion concentration was determined with a calcium selective electrode model F2112Ca with calomel reference electrode K401 and appropriate meter PHM82 (Radiometer A/S, Copenhagen, Denmark), and readings were recorded with a chart recorder. The system was calibrated with $CaCl_2$ solutions in the same buffer media (0.15 M NaCl and 0.01 M HEPES) prepared by volumetric additions. Particle growth kinetics were determined by using a model LS-5 (Perkin-Elmer, Oak Brook, IL) fluorescence spectrometer as a fixed angle scattering photometer by setting both emission and excitation wavelengths to 500 nm and both slit widths to 5 nm. Polystyrene cuvettes were used as sample cells. The scattered intensity was minimal from the original solutions, but rose rapidly with the appearance of crystals in the sample. No attempt has been made to quantitate this response in terms of particle number, size and distribution since the purpose of this experiment was to test for changes in the kinetics, i.e., nucleation and growth, of CaOx crystals. Again, time dependent signals were recorded with a chart recorder and digitized for presentation.

X-ray powder diffraction was performed on thirty samples selected from various solution compositions at the National VA Crystal Identification Laboratory (Milwaukee, WI) to confirm the morphological identification. In general, microscopic examination of these samples was a much more sensitive measure of composition than powder diffraction, allowing the identification of even a single crystal of the non-dominant structure in a field of thousands of the other type. In fact, no conditions were found to be purely one crystalline structure or the other in microscopic examination. However, samples were considered to be pure in one structure if only a few crystals, representing a trivial number fraction, of the other structure were seen after examining the entire area of the slide. Powder diffraction results were used for samples demonstrating an ambiguous morphology (e.g., equimolar with SS = 15.6 and with 616 nM PA). This protocol was used throughout the experiment.

We calculated the SS by the following definition:

$$SS = \{([Ca][Ox])/([Ca]_0[Ox]_0)\}^{0.5}$$

where [Ca] and [Ox] represent the initial ion concentrations for calcium and oxalate ions, respectively, in a given solution and $[Ca]_0$ and $[Ox]_0$ are the concentrations of those ions at equilibrium (calculated to be 0.15 mM for the temperature and buffer conditions above, using the speciation program EQUIL2 [20]). This quantity is more properly defined as the above ratio of activities; however, the solution ionic strength and pH conditions are dominated by the NaCl and HEPES buffer components, with relatively small variations in the Ca and Ox concentrations. Consequently, the correction factors to calculate ionic activities are expected to cancel with a very small error.

Results

In Figures 1, 2 and 3, examples of representative fields for three samples are shown to illustrate the typical crystal habits seen for COM rich (Fig. 1, from a solution with a Ca:Ox ratio of 10:1, at SS = 10.5 with no PA added), COD rich (Fig. 2, from an equimolar sample at SS = 9.9 with 123 nM PA added) samples, and mixed fields (Fig. 3, from an equimolar sample at SS = 13.2 with 123 nM PA added). All three micrographs were taken from fields where the crystals had washed off the surface of the filter for clarity of presentation.

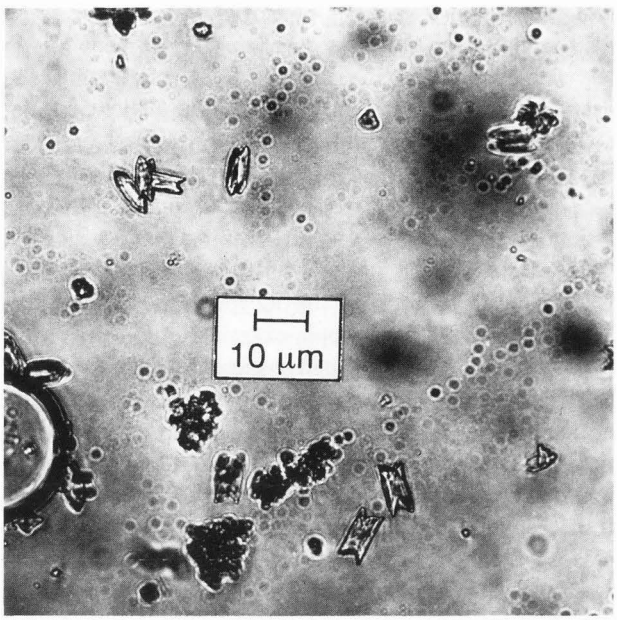

Figure 1. Optical micrograph of COM morphology typical of crystals grown with no PA added. This sample resulted from the precipitation from 5.0 mM Ca with 0.5 mM Ox and no PA added (SS = 10.5).

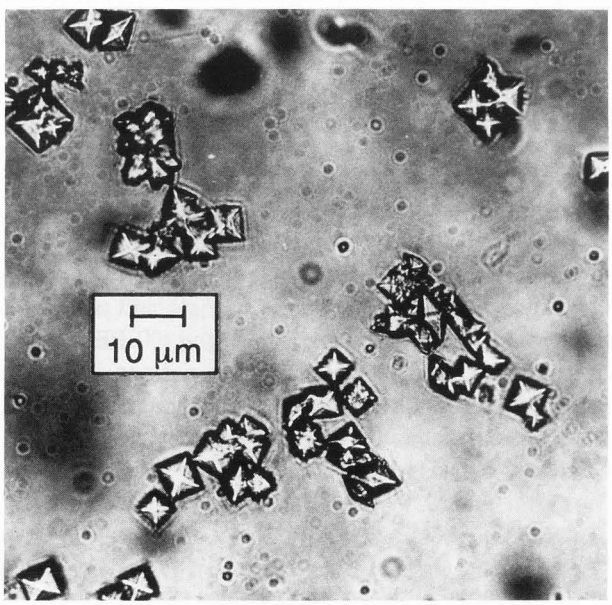

Figure 2. Optical micrograph of COD morphology typical of crystals grown with a large concentration of PA. This sample resulted from the precipitation of 1.5 mM Ca with 1.5 mM Ox and 123 nM PA (SS = 9.9).

No differences were discernible between crystals that remained on the filter and those that washed off.

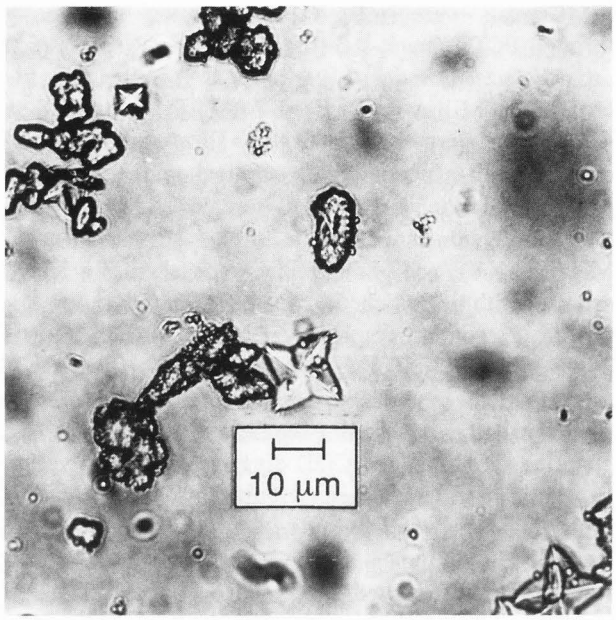

Figure 3. Optical micrograph of mixture of COM and COD morphologies formed simultaneously in the presence of intermediate concentrations of PA. This sample resulted from the precipitation of 2.0 mM Ca with 2.0 mM Ox and 123 nM PA (SS = 13.2). The "starfish" geometry of COD is seen near the center of Figure 3, and it has a maximum linear dimension of about 15 μm. Note that this condition was at the same quantity of added PA as shown in Figure 2, but at this higher SS, the PA concentration was no longer sufficient to lead to complete COD formation.

The plate-like forms seen in Figure 1 were characteristic of the COM crystals formed under most conditions, although, at high supersaturations, the crystals became somewhat rounded at the ends and appeared to be a bit thicker with a dimpling of the central portion suggestive of a "canoe" shape, as described previously [10]. Several crystals in Figure 3 show these characteristics. The long axis of these crystals was typically in the range of 5 to 20 μm. In many samples, aggregates of plates were observed. Morphologic characterization was confirmed by X-ray powder diffraction for any variations observed. While some variation of COM crystal morphology was observed at different conditions, COD morphology was always as seen in Figures 2 and 3.

In Figure 2, the octahedral crystals characteristic of COD are seen. Again, these crystals were usually in the size range of 5 to 20 μm in maximum dimension. In Figure 3, not only are COM and COD forms seen, but also a distorted octahedral form that looks like a four-armed starfish. These were demonstrated to be COD structures, likely a resultant from twinning, and were

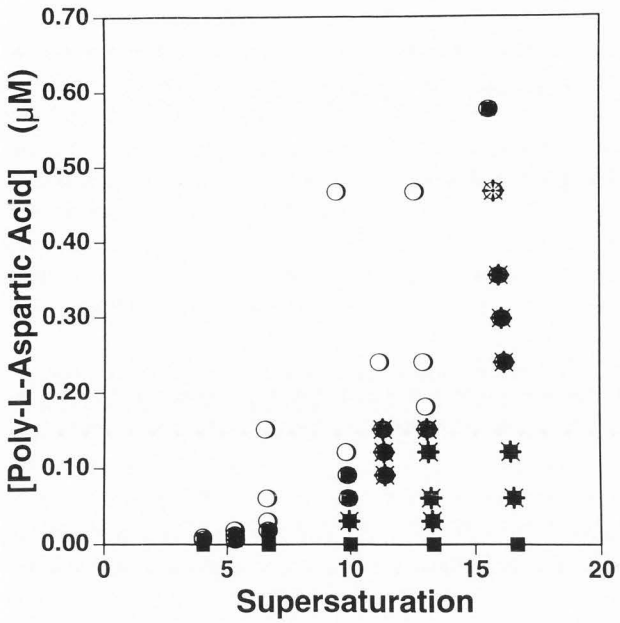

Figure 4. Crystal composition phase diagram for equimolar CaOx solutions, with the supersaturation plotted along the abscissa and the concentration of PA on the ordinate. The presence of COM crystals is indicated by a filled square, while COD is indicated by an open circle. The "starfish" COD geometry is represented by an eight-pointed star. Superimposed symbols at many intermediate conditions indicate the formation of both COM and COD structures simultaneously at those conditions.

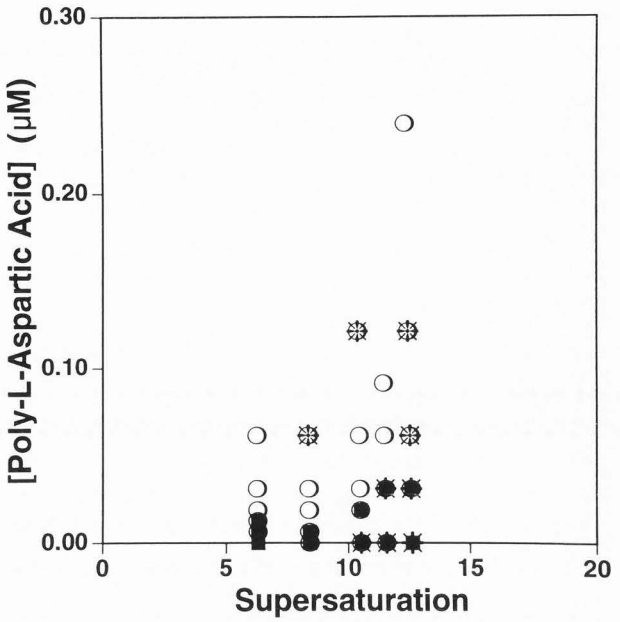

Figure 5. Crystal composition phase diagram for solutions with a ratio of Ca:Ox of 10:1 plotted as in Figure 4. Filled square: COM crystals; open circle: COD crystals; eight-pointed star: "starfish" COD geometry.

---

most commonly observed in samples with intermediate amounts of PA added and at higher SS. These crystalline forms tended to be slightly larger than the classic COD forms, ranging up to about 25 μm in maximum dimension, and they were frequently the first COD forms seen with increasing concentration of PA.

There is a population of crystals seen in all three examples above that are too small to be adequately characterized by optical microscopy and clearly much smaller than the 5.0 μm pore size of the filter. Since the particle size distributions were inherently broad, these were felt to be representative of the compositional distribution of the larger crystals seen. The small crystals appeared to be a very small fraction of the total crystal mass by optical microscopy, although these were collected on a 5.0 μm filter. To better gauge the significance of this population of crystals in terms of weight fraction of the total sample, a comparison was made between the crystal mass isolated with a 5.0 μm filter versus that obtained with a 0.1 μm filter. We observed 1.15 mg (SD 0.06) recovered with a 5.0 μm filter and 1.18 mg (SD 0.10) recovered with a 0.1 μm filter from equimolar calcium oxalate solutions at SS = 9.9 with 62 nM PA at 27 hours (recovered crystal mass was the same at 4 hours). No significant difference was observed. Given the uncertainties in weighing, we placed the unrecovered weight fraction with a 5.0 μm filter at < 0.05. It is important to note that X-ray powder diffraction data did not show evidence of unrecognized crystal structures (either COD in a sample felt to be pure COM, or vice versa), suggesting that these small crystals were at least the same structure as the larger crystals, if not a trivial weight fraction of the total sample. In either case, further characterization of them would not affect our general conclusions, so further evaluation (e.g., by scanning electron microscopy) was not pursued.

The crystal composition phase diagram for equimolar Ca and Ox is shown in Figure 4 as a function of SS and [PA]. COM (filled squares) was formed exclusively in the absence of PA. At sufficiently large [PA], at most SS (i.e., $>$ 100 nM PA at SS = 10), COD (open circles) was formed exclusively. The symbols were chosen in a manner to highlight the concentration of PA above which COM was no longer observed. At low SS, i.e., 6 or below, the points are too closely spaced on this scale to show it clearly, but the same qualitative picture was demonstrated. With no added PA, the samples were pure COM, but pure COD was obtained by the addition of 9.2 nM PA at SS of 4 and 18 nM PA at SS of 5.3. A similar result was obtained by reducing the SS at constant added PA, as illustrated in Figures 2 and 3.

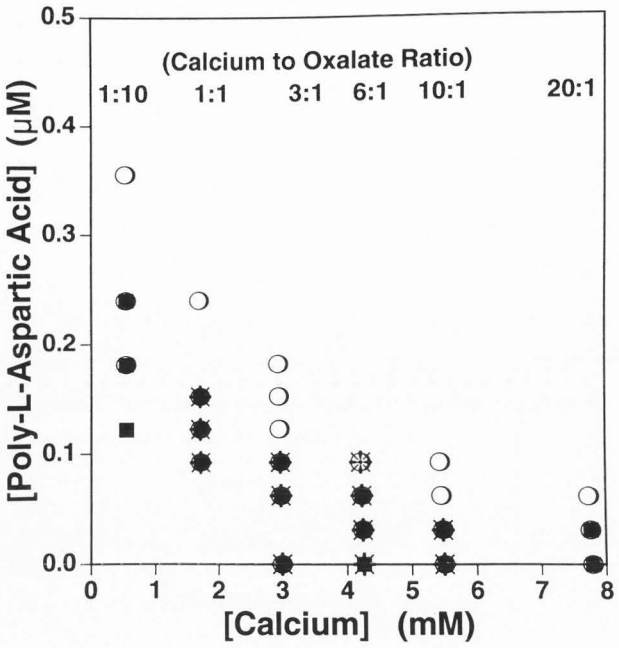

Figure 6. Crystal composition phase diagram for solutions at constant SS of 11.58 ± 0.05, but with varying ratios of Ca:Ox. Ca concentration is plotted along the abscissa, with the matching Ca:Ox ratio listed at the top of each data column. The PA concentration is plotted on the ordinate. Filled square: COM crystals; open circle: COD crystals; eight-pointed star: "starfish" COD geometry.

The highest SS data apparently deviate from the pattern, but this must be interpreted cautiously, given the kinetic limitations of our experimental design, as described above. The increase in the [PA] required to obtain COD with increasing SS was dramatic.

At intermediate [PA], crystals of both types were observed, and these regions are identifiable by the superposed symbols for various crystalline forms. The starfish form of COD (eight-pointed character) was also found at high SS and intermediate amounts of PA (i.e., SS > 10 and 100 nM PA). The relative ratio of COD to COM was seen to increase systematically with the amount of PA added. This behavior was also demonstrated at the highest SS, even though a condition showing pure COD was not clearly identified. Although no effort was made to quantitate the relative amount of COD as a function of [PA], clearly, the transition from favoring one crystalline form to favoring the other was a gradual one, indicating a proportional response of crystal structure to [PA]. The angulation of the data toward the ordinate in the columns of nearly constant supersaturation resulted from correcting for the dilution from adding the PA stock solution.

This general pattern was reproduced at other Ca:Ox ratios, although as this ratio increased, the amount of PA required to obtain pure COD decreased. Figure 5 shows the comparable crystal composition phase diagram at a Ca:Ox ratio of 10:1. The same symbolic representation of data has been used to facilitate comparison of data. One clear difference at higher Ca:Ox ratios was the presence of significant, though still small, amounts of COD crystals in samples with no PA added, consistent with the reduced need for PA to obtain COD. This was more prominent at higher SS.

Figure 6 shows the dependence of crystal structure on the Ca:Ox ratio and the amount of PA added for a SS of 11.58 ± 0.05, using the same symbolic representations as above. The data are shown according to the interpretation by optical microscopy. The sample at 0.55 mM Ca and 360 nM PA had a significant, minor fraction of the crystal mass with ambiguous morphology. Subsequent X-ray powder diffraction demonstrated that COM was present in this sample, so the upward curvature suggested by this diagram at low Ca:Ox ratios, i.e., 1 or less, is certainly greater than that indicated in Figure 6. While our experiment emphasized the behavior under normal urine conditions, which is fully included in the range of Ca:Ox ratios sampled here, the dependence on Ca:Ox ratio is strongest at the lower extreme of the data range. At the higher extreme, the amount of PA required for formation of COD is apparently independent of Ca:Ox ratio.

The effect of monomeric L-aspartic acid was also examined at equimolar conditions and SS = 6.7. Crystals were grown in the presence of 5 μg/ml and 10 μg/ml of added aspartic acid monomer (corresponding on a weight basis to the 0.33 and 0.66 μmolar PA solutions), and the crystals obtained were indistinguishable from those grown in the absence of any added inhibitors; i.e., pure COM. With the equivalent mass of PA, COD was found at either of these concentrations (see Fig. 4). Aspartic acid monomer may be an inhibitor at higher concentrations, similar to citrate and pyrophosphate anions, but it is clearly less effective than PA in this regard. Evidently, the polymeric nature of the inhibitor is a critical characteristic for the effects on crystal structure demonstrated above.

To better understand the mechanism of the PA effect on CaOx crystallization, two additional experiments were performed. A calcium selective electrode was used to test for a decrease in the Ca ion activity with addition of PA. The electrode was calibrated over the range of 0.1 mM to 10 mM Ca ion with a nearly linear increase in voltage output per unit change in log([Ca]); slope = 30 mV/decade and intercept = 43 mV with [Ca] ion expressed in mM units. No difference was detectable in the [Ca] ion at 1.0 mM between the presence or absence

of 616 nM PA. The minimum detectable change was expected to be 0.5 mV based on the variation in recorded potentials for independently prepared solutions, or about a 4% change in the [Ca]. The [PA] corresponds to 0.068 mM aspartic acid monomer units, so a detectable change even at this largest [PA] tested would require condensation of Ca ion on the chain past neutrality. Clearly, for the quantities of PA used in this study, there was no appreciable effect on the Ca ion activity by the addition of PA.

In a second experiment, the influence of [PA] on the kinetics of COD crystallization was probed. Equimolar solutions at 1.5 mM Ca and Ox (SS = 9.9) were prepared at four quantities of added PA: 0 nM, 123 nM, 246 nM and 492 nM. COM was formed with no added PA, while the other three conditions lead to COD; the 123 nM condition was near to the lower boundary for complete COD formation. The time dependence of the scattered intensity is shown in Figure 7 for four representative precipitations. Data were not obtained during the first 60 seconds due to mixing and solution transfer issues. There was a clear progression toward longer lag times with increasing [PA], and there appeared to be a decrease in the initial slope. The increasing lag times indicate an increasing delay in or slowing of nucleation. The changes in the initial slope are likely related to differences in growth rates, but this conclusion is tenuous given the known dependence of scattered intensity on the number, size and shape of the growing crystals, and none of these parameters were measured independently.

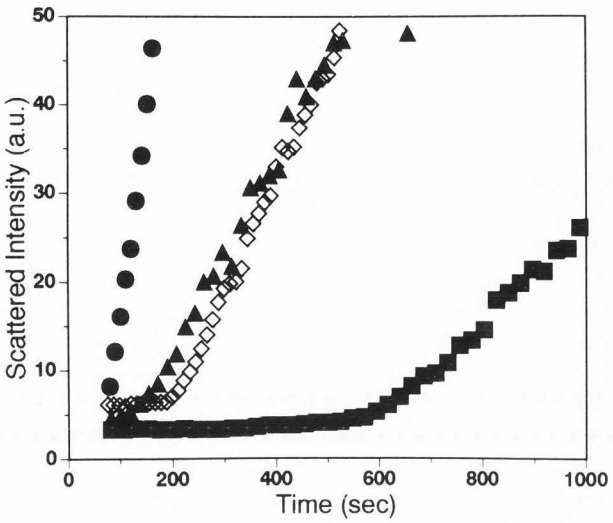

Figure 7. The scattered intensity as a function of time from solutions of 1.5 mM Ca with 1.5 mM Ox and varying amounts of added PA is plotted. Filled circle: no added PA (formed COM); filled triangle: 123 nM PA (formed COD); open diamond: 246 nM PA (formed COD); filled square: 492 nM PA (formed COD). Data for the first 60 seconds was not obtained due to limitations in our ability to mix the solutions and transfer them to the instrument. Scattering was measured in a fluorescence spectrometer at a wavelength of 500 nm.

Discussion

The data presented above do not elucidate the mechanism of the interaction of PA with the growing crystal mass that leads to the preferential formation of COD, but several significant clues are evident.

There is a dramatic increase in PA requirement for COD formation with increasing SS, implying a relationship between the number of nuclei and the amount of polymer added. Unfortunately, quantitative data for the number of nuclei formed under the various conditions tested in this study are not yet available to allow a direct comparison of the increase in PA with the increase in number of crystal nuclei per unit volume. The gradual transition from predominantly COM to predominantly COD with increasing PA at a constant SS also suggests a relationship between the polymer concentration and the number of growing crystals or nuclei. The proportional response to PA implies that PA must somehow be consumed in this process, either through binding to a non-propagating COM nucleus or adherence to a COD crystal. Other reported inhibitors also demonstrate a proportional response [16].

There was no evidence for conversion of one structure to the other, in particular COM to COD, in our observations. No difference was noticeable in the crystal composition (COM:COD ratio) between samples crystallized for several hours and samples crystallized for several days, although a transition from COD (a metastable structure) to COM might occur on a longer time scale or under other conditions. Tested in a second way, if the PA addition was made after Ox was added to initiate the precipitation at a condition that would normally yield pure COD (e.g., equimolar at 1.5 mM Ca and Ox; SS = 9.9 with 308 nM PA), a mixture of COM and COD was obtained, providing that the addition of PA was delayed until some crystal mass had formed in the sample. Evidently, PA does not transform the COM structure to COD, but it does prevent further development of COM, despite the presence of COM "seed" crystals in the precipitating solution. Others have proposed that COD forms first and is then converted to COM [19], but we saw no evidence to support this interpretation in our experiments.

We favor the interpretation that the presence of PA inhibits the growth of both COM and COD, but is more effective against COM formation, so that COD becomes the favored product for kinetic reasons. The study [16]

cited above reported that kinetic inhibitors of COM favor COD formation, including urinary solutes, heparin, RNA and small molecule inhibitors, such as citrate and pyrophosphate. Another study [9] demonstrated that a micellar anionic surfactant also inhibited crystal formation and favored the formation of COD in a spontaneous nucleation experiment, while non-ionic and cationic micelles did not affect the crystal structure, although they did influence crystallization kinetics (non-ionic micelles facilitating and cationic micelles inhibiting crystallization). It is unlikely that these disparate compounds and PA all manage to form a unique template surface to stimulate the formation of the less favored COD structure. However, they are all anionic (or polyanionic), and could be expected to condense on a cationic growing crystal surface in a similar manner, possibly inhibiting the growth of that surface. The relatively greater effectiveness of the polyanions would be consistent with their inherently greater affinity through cooperativity for an oppositely charged surface in this model, and with the possibility that binding of one macromolecular structure might cover the entire growing surface of an incipient nucleus. Why PA and other inhibitors would be more effective against COM than COD is not evident at this time, but it must certainly depend on the surface characteristics of growing crystal faces.

An additional inference can be made from the behaviors observed as a function of Ca:Ox ratio, with respect to the relative merits of the template and inhibitor models. Template growth should be favored by low Ca (high Ox) conditions. If PA was acting as a template, the first layer of ion condensation must be Ca. Since the template generated structure (COD) must compete for available Ca (and Ox) with spontaneous nucleation which leads to COM, the natural ionic association of Ca with PA could create locally high concentrations of Ca, fostering template stimulated crystal formation at the expense of spontaneous nucleation (COM formation). On the other hand, a large excess of Ca ion could saturate the template sites, while still maintaining a large solution Ca concentration to drive spontaneous nucleation and COM formation, predicting an increased requirement for PA with increasing Ca:Ox ratio. Of course, PA must still be serving as an inhibitor of both COD and COM growth at the same time it is serving as a template. Conversely, in the inhibitor model, PA must compete for the appropriate growing crystal face with other anions in solution (monomeric and polymeric), and its inhibitory effect should be reduced in the presence of sufficiently high [Ox], through a competitive equilibrium process. The cooperative binding advantage of PA is proportional to the number of monomer units per chain, but each carboxylic acid end group should have essentially the same affinity for the charge sites on crystal nuclei, whether from PA or Ox. The high Ox conditions reported here correspond to approximately a 100-fold excess of Ox to aspartic acid monomer units at the highest [PA] used. Low Ox (high Ca) conditions should then facilitate the effect of PA on crystal structure. Our data, in Figure 6, clearly agree with the inhibitor model. This is also consistent with *in vivo* data showing that high [Ca] favors COD in crystalluria [6].

We conclude that the inhibitor model of interaction is much more consistent with the available data. Since COD can spontaneously form in solution at least at high Ca concentrations, the differential change in the growth rate of COM relative to COD may not need to be very large to lead to preferential COD formation. However, we cannot exclude the possibility that the polymer induces a change in the structure of the ionic cluster corresponding to the incipient crystal nucleus that allows it to grow as a COD crystal, instead of COM, but this hypotheses fits less well with our data and with the published effects of other inhibitor molecules. Other mechanisms may also be possible. The implications for kidney stone disease may be significant, if subsequent experiments show a preferential formation of COD in the presence of normal urinary macromolecules-like uropontin and a reduced affinity of COD for renal tubule cells, compared to COM.

In summary, we have shown that PA, a model polyanion inhibitor of calcium oxalate crystal growth, favors the formation of COD in supersaturated solutions of calcium and oxalate at pH = 7.5 and 0.15 M NaCl. The concentration of PA required to cause this change in preferred crystal structure increases with increasing supersaturation and decreases with increasing Ca:Ox ratio, in a nonlinear manner in both instances. Also, the formation of COD is inherently favored by high Ca:Ox ratios. The transition of crystalline forms is a smoothly varying function of PA concentration, implying a stoichiometric relationship to COM (or COD) crystal mass. PA has also been shown to inhibit the kinetics of COD crystal nucleation and growth. The effect of PA on the crystal structure depends on the polymeric nature of the molecule, as monomeric aspartic acid has no effect on crystal structure or morphology at similar mass concentrations.

Acknowledgments

This work was supported by the department of Veteran Affairs Medical Research Service and by research grants DK-41725 and DK-48504 from the National Institutes of Health. We gratefully thank Mrs. Kathy Fryjoff and Dr. Neil Mandel for their assistance in performing X-ray powder diffraction analyses. We also appreciate helpful discussions with Drs. Jack Kleinman and John Wiessner, and the assistance of Mrs. Ann Beshensky.

References

[1] Addadi L, Weiner S (1985) Interactions between acidic proteins and crystals: Stereochemical requirements in biomineralization. Proc Natl Acad Sci **82**: 4110-4114.

[2] Bunker BC, Rieke PC, Tarasevich BJ, Campbell AA, Fryxell GE, Graff GL, Song L, Liu J, Virden JW, McVay GL (1994) Ceramic thin-film formation on functionalized interfaces through biomimetic processing. Science **264**: 48-55.

[3] Butler WT (1989) The nature and significance of osteopontin. Connect Tissue Res **23**: 123-136.

[4] Coe FL, Parks JH, Asplin JR (1992) The pathogenesis and treatment of kidney stones. New Engl J Med **327**: 1141-1152.

[5] Denhardt DT, Guo X (1993) Osteopontin: A protein with diverse functions. FASEB J **7**: 1475-1482.

[6] Elliot JS, Rabinowitz IN (1980) Calcium oxalate crystalluria: Crystal size in urine. J Urol **123**: 324-327.

[7] Fellstrom B, Danielson BG, Ljunghall S, Wikstrom B (1986) Crystal inhibition: The effects of polyanions on calcium oxalate crystal growth. Clin chim Acta **158**: 229-235.

[8] Fleisch H (1978) Inhibitors and promoters of stone formation. Kidney Int **13**: 361-371.

[9] Furedi-Milhofer H, Tunik L, Bloch R, Garti N (1994) The influence of surfactants on the crystallization of calcium oxalate hydrates. Mol Cryst Liq Cryst **248**: 199-206.

[10] Grover PK, Ryall RL, Marshall VR (1990) Does Tamm-Horsfall mucoprotein inhibit or promote calcium oxalate crystallization in human urine? Clin chim Acta **190**: 223-238.

[11] Ito H, Coe FL (1977) Acidic peptide and polyribonucleotide crystal growth inhibitors in human urine. Am J Physiol **233**: F455-F463.

[12] Mandel N (1994) Crystal-membrane interaction in kidney stone disease. J Am Soc Nephrol **5**: S37-S45.

[13] Mandel NS, Mandel GS (1989) Urinary tract stone disease in the United States veteran population. I. Geographical frequency of occurrence. J Urol **142**: 1513-1515.

[14] Mandel NS, Mandel GS (1989) Urinary tract stone disease in the United States veteran population. II. Geographical analysis of variations in composition. J Urol **142**: 1516-1521.

[15] Mandel N, Riese R (1991) Crystal-cell interactions: Crystal binding to rat renal papillary tip collecting duct cells in culture. Am J Kidney Dis **17**: 402-406.

[16] Martin X, Smith LH, Werness PG (1984) Calcium oxalate dihydrate formation in urine. Kidney Int **25**: 948-952.

[17] Pierratos AE, Khalaff H, Cheng PT, Psihramis K, Jewett MAS (1994) Clinical and biochemical differences in patients with pure calcium oxalate monohydrate and calcium oxalate dihydrate kidney stones. J Urol **151**: 571-574.

[18] Shiraga H, Min W, VanDusen WJ, Clayman MD, Miner D, Terrell CH, Sherbotie JR, Foreman JW, Przysiecki C, Neilson EG, Hoyer JR (1992) Inhibition of calcium oxalate crystal growth *in vitro* by uropontin: Another member of the aspartic acid-rich protein superfamily. Proc Natl Acad Sci **89**: 426-430.

[19] Tomazic BB, Nancollas GH (1979) A study of the phase transformation of calcium oxalate trihydrate-monohydrate. Invest Urol **16**: 329-335.

[20] Werness PG, Brown CM, Smith LH, Finlayson B (1985) EQUIL2: A BASIC computer program for the calculation of urinary saturation. J Urol **134**: 1242-1244.

[21] Wiessner JH, Mandel GS, Mandel NS (1986) Membrane interactions with calcium oxalate crystals: Variation in hemolytic potentials with crystal morphology. J Urol **135**: 835-839.

[22] Wiessner JH, Kleinman JG, Blumenthal SS, Garansic JC, Mandel GS, Mandel NS (1987) Calcium oxalate crystal interaction with rat renal inner papillary collecting tubule cells. J Urol **138**: 640-643.

[23] Worcester EM, Beshensky AM (1995) Osteopontin inhibits nucleation of calcium oxalate crystals. Ann NY Acad Sci **760**: 375-377.

[24] Worcester EM, Blumenthal SS, Beshensky AM, Lewand DL (1992) The calcium oxalate crystal growth inhibitor protein produced by mouse kidney cortical cells in culture is osteopontin. J Bone Miner Res **7**: 1029-1036.

Discussion with Reviewers

L. Addadi: The "starfish" form of COD is treated as a separate and important observation. This is, in my opinion, just an effect of twinning that has been observed repeatedly in the literature of COD and is a very common event in crystal growth.

G.H. Nancollas: The X-ray powder diffraction of the "starfish" crystallites will be important.

Authors: We agree with the description of this "starfish" structure as a twinned COD crystal, but we have not seen any published examples or description of conditions favoring its formation. We deduced the crystal structure for this form by the following finding. We examined a sample (equimolar; SS = 13.2, 123 nM PA) which was a mixture of "starfish" and normal COM forms (no apparent normal COD forms) by microscopy; we found the sample to be a mixture of COM and COD by powder diffraction.

H.-G. Tiselius: The quantitation of the relative occurrence of COD and COM crystals in the precipitate is of

crucial importance and in view of the great number of crystals, particularly at high levels of SS, it can be assumed that this is not easy. A detailed description of how the authors coped with this problem is desirable.

G.H. Nancollas: Did the authors use the X-ray diffraction technique in order to determine the exact percentage of COM and COD? This can easily be achieved with appropriate attention to standardization. This is particularly true in interpreting the data shown in Figures 4 and 5; it should be possible to quantify the amounts of different hydrates formed as a function of PA concentration.

L.C. Cao: The designed and used model system *in vitro* is semi-quantitative since neither light microscopy or X-ray powder diffraction can give an accurate result about COM/COD ratio.

Authors: We specifically avoided the question of numerical quantitation of the fractions of COM and COD in these samples because of the difficulty in obtaining these data. Dr. Neil Mandel, who is head of the National VA Crystal Identification Center in Milwaukee and who donated the X-ray powder diffraction analyses to our work, advised us that the use of powder diffraction for quantitative analysis was possible, but extremely difficult, typically yielding data of limited precision. This comment is echoed by Dr. Cao above, while Profs. Nancollas and Tiselius are advocating powder diffraction for this purpose. We defer any conclusions of the validity of this analytical method to these people since we are not experts in this technique. Digital image analysis was a second possibility, but unfortunately, it is not available to us here. We are currently investigating the use of Fourier-transform infrared spectroscopy (FTIR) for bulk compositional analysis of calcium oxalate crystals, but it too has limitations that we have not yet completely resolved. Consequently, we emphasize the point that the addition of polyaspartate to the precipitation leads to a structural change in the crystal formed. We also note that the response to polyaspartate is a gradual one with the addition of increasing amounts of polymer. Both of these points are unambiguously made with our experiments. While we did not determine the functional dependence of crystal composition on polyaspartic acid addition, Martin *et al.* [16] showed essentially a linear increase in COD with added inhibitors (both monomeric and polymeric), and we anticipate a similar behavior for our inhibitor based on our visual impression.

H.-G. Tiselius: In these experiments, did you, under any conditions, observe crystals of calcium oxalate trihydrate (COT)?

Authors: We did not find COT at any of the conditions reported here. We have grown COT in our laboratory, but only when stirring the samples with a magnetic stirring apparatus, with little or no inhibitor present.

G.H. Nancollas: One has to be careful in identifying phases by morphology. The crystals in Figure 1 appear to be significantly twinned. Did the authors measure the particle size distribution of the precipitated products since some appear to be more aggregated than others? Aggregation may well be a significant factor in the pathological formation of calcium oxalate deposits.

Authors: We agree that aggregation may be an important physiological issue, and we certainly see evidence of it in our *in vitro* studies. However, we did not specifically follow this parameter since our focus was on crystal structure in this study. When the crystal morphology did not allow for a straightforward identification of the structure (which occurred in very few cases in our experiments), we used powder diffraction as our absolute identification method.

G.H. Nancollas: It is important to recognize that the crystal surface potential (zeta) will be sensitive both to the adsorption of excess calcium ions and the adsorption of PA. These will be opposing effects on the zeta potential and also on the degree of aggregation. The fact that monomeric aspartic acid has no influence on the phase formed again suggests that the surface potential may be an important parameter to monitor.

Authors: We agree that the surface zeta potential is likely a critical parameter in determining the crystal interaction. These experiments would probably help elucidate the nature of the polymer-crystal interaction, but they are beyond the scope of this study.

S.R. Khan: Have you examined the impact of osteopontin on calcium oxalate crystal formation *in vitro* and compared it with the effect of PA?

Authors: We are currently conducting experiments to examine the influence of several macromolecules found in urine, including osteopontin, on the crystal structure of calcium oxalate crystals formed under similar conditions to those reported here. Osteopontin also affects the crystal structure in a similar manner at physiologically relevant concentrations. These experiments will be described in detail in a subsequent publication.